Journal of Physical Organic Chemistry

WILEY

Journal of Physical Organic Chemistry

RESEARCH ARTICLE OPEN ACCESS

False Identification of (Anti)aromaticity in Polycyclic Molecules in Ground and Excited States Through Incorrect Use of NICS

Péter J. Mayer | Henrik Ottosson

Department of Chemistry – Ångström Laboratory, Uppsala University, Uppsala, Sweden

Correspondence: Henrik Ottosson (henrik.ottosson@kemi.uu.se)

Received: 31 October 2024 | **Revised:** 18 December 2024 | **Accepted:** 6 January 2025

Funding: This work was supported by Vetenskapsrådet (2023-04179) and Carl Tryggers Stiftelse för Vetenskaplig Forskning (22: 2330).

Keywords: antiaromaticity | aromaticity | Baird's rule | excited-state aromaticity | NICS pitfalls

ABSTRACT

Aromaticity is a key concept in physical organic chemistry. However, as it cannot be measured directly, it is assessed indirectly via other properties (energetic, electronic, geometric and magnetic). Although these properties describe aromaticity, they are not solely related to aromaticity as the observed values also can stem from, for example, magnetically induced local currents at certain atoms or groups, or strain in the σ-skeleton. This can lead to misinterpretations. Here, we highlight a pitfall in the (anti) aromaticity assessment of polycyclic molecules when it is mainly based on nucleus independent chemical shifts (NICSs). The NICS index can be misinterpreted to indicate 'aromaticity' or 'antiaromaticity' in nonaromatic rings as a result of paratropic or diatropic ring currents in adjacent rings. We explore if such false indications by NICS are (i) stronger in Baird-aromatic or -antiaromatic excited states (mainly triplet and quintet, but also singlet) than in closed-shell singlet ground states, and (ii) if a paratropic ring current in an adjacent ring causes stronger or weaker false 'aromaticity' than a diatropic one causes false 'antiaromaticity'. Based on our computations we conclude that larger aromatic rings in all types of states (e.g., a triplet state Baird-aromatic cyclooctatetraene ring) have greater influence than smaller ones, yet, we see no indication that the effect is stronger in excited states. Instead, annulene rings are more influential in their paratropic (antiaromatic) states, regardless if ground or excited states, than in their diatropic (aromatic) ones.

1 | Introduction

Aromaticity can be used as a tool to rationalise reactivity and many other properties of organic molecules [1–5]. The most common type, Hückel-aromaticity, comes from delocalisation of $4n+2\pi$-electrons in annulenes [6]. The counter-concept, antiaromaticity, was introduced by Breslow, who stated that conjugation in $4n\pi$-electron annulenes leads to destabilisation [7]. In the lowest $\pi\pi^*$ excited triplet state (T_1), the electron counting rules for aromaticity and antiaromaticity are opposite to what they are in the closed-shell singlet ground state (S_0), meaning that cycles with $4n$ π-electrons become aromatic, while those with $4n+2$ are antiaromatic in that state [8]. This relationship is now known as Baird's rule [9], and for several compounds it has been found to be valid also in the lowest singlet excited $\pi\pi^*$ state (S_1) [10–12].

In aromatic molecules, the following properties are observed: (i) higher thermodynamic stability compared to isomers with the same amount and type of bonds, (ii) π-electron delocalisation, (iii) bond length equalisation and (iv) induction of a diatropic ring current running through the complete cycle when the molecule is placed in an external magnetic field (Figure 1A). These properties are observables, but they have

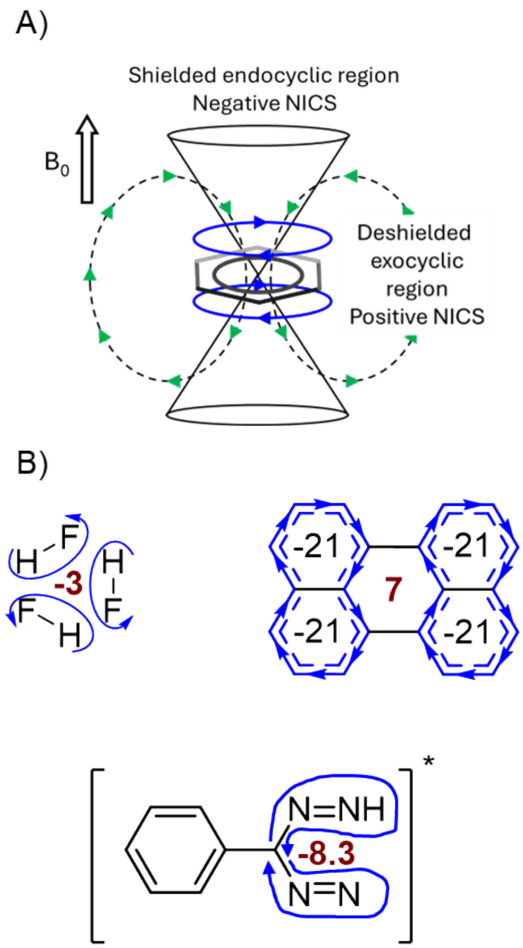

FIGURE 1 | Magnetically induced ring currents (also local ones) and their (de)shielding influence. (A) Magnetic shielding cone resulting from the magnetically induced diatropic ring current of benzene in S_0 (inner blue circular arrows), and an illustration of how it affects the NICS values. (B) Examples of NICS values (bold red values) that result from neighbouring magnetically induced currents (blue arrows), and which falsely suggest 'aromaticity' or 'antiaromaticity' [23, 26–28].

their pros and cons when used for (anti)aromaticity assessments [13, 14]. The fact that aromaticity cannot be directly observed can lead to misinterpretations, and potentially to wider misconceptions if the misinterpretations are not addressed and reinterpreted. When exploring (anti)aromaticity effects in electronically excited states it is especially important to (i) realise the limitations, complications, and pitfalls of the excited-state (anti)aromaticity concept itself, (ii) assess the potential (anti)aromaticity by several different types of descriptors and (iii) put up and validate alternative qualitative models that may rationalise the computational observations [15]. For example, a computed aromatic character of a complex molecule in its lowest excited states is not necessarily due to Baird-aromaticity as such a molecule may instead exhibit Hückel-aromaticity in these states [16], or it may simultaneously have Hückel- and Baird-aromatic characters [17, 18].

Exclusive use of the most common magnetic (anti)aromaticity indicator, nucleus independent chemical shifts (NICSs) [19, 20], can lead to misinterpretations if the limitations and pitfalls of this index are ignored. This is due to the non-local (extensive) nature of the magnetic shielding around a cyclic molecule or molecular segment that exhibits an induced current density (e.g., a ring current) when placed in a magnetic field. The NICS value is simply the negative of the shielding at the particular point in space considered. With regard to a magnetically induced ring current in an aromatic cycle, it causes a magnetic shielding in the middle of the ring and a deshielding on its outside (Figure 1A) [21]. The opposite is observed for antiaromatic cycles. Thereby, the calculated NICS values on the outside of an aromatic or antiaromatic ring (which we refer to as exocyclic) have opposite sign to those on the inside, regardless if that 'outside' happens to be inside a nonaromatic ring. Noteworthy, from a single NICS value, or even a set of such values, one cannot uniquely reverse-engineer the magnetically induced current densities (MICDs) which are the responses of the molecules to the external magnetic field [22]. Yet, despite that the current densities cannot be uniquely regained from the NICS values, simpler bond currents can be reverse-engineered from them [23]. These bond currents contain the information required to explore the tentative (anti)aromatic character of (poly)cyclic molecules.

NICS results have been debated and scrutinised for long [24, 25], even though faulty (anti)aromaticity assessments often stem from insufficient insights on the limitations and pitfalls by the users of the NICS methodology. It was found early on that the cyclic hydrogen-bonded trimer of hydrogen fluoride, $(HF)_3$, has a negative NICS value of −3 ppm in the middle of the hexagon (Figure 1B). Due to this, the $(HF)_3$ complex was first claimed to be aromatic [26]. However, this alleged aromaticity was subsequently disproven by calculations of the MICDs which revealed that the negative NICS resulted from local circulations in the induced current density at the three individual HF molecules (Figure 1B) [27]. When combined these give a similar shielding at the centre of the $(HF)_3$ complex as a proper diatropic ring current. Another example comes from perylene where the middle hexagon exhibits a 7 ppm $NICS(1.25)_{zz}$ value (Figure 1B). Based on this NICS value, this cycle may at first glance be assessed as weakly antiaromatic, however, there is no induced paratropic ring current that generates the positive NICS value [23]. Instead, the value stems from induced diatropic ring currents in the two naphthalene moieties that surround the central hexagon. Nonzero NICS values without proper ring currents have also been observed in electronically excited states. For a reaction intermediate formed in the photodissociation of phenyltetrazoles (Figure 1B), one calculated a $NICS(1)_{zz}$ value of −8.3 ppm for the partially dissociated tetrazole ring. At a first look, this would be assigned as 'aromatic', but no proper ring current could be observed (Figure 1B), only currents in a semi-circle [28]. While further cases have been reported [29], these three examples illustrate how NICS can be used incorrectly as an aromaticity descriptor. Knowledge on the pitfall is also relevant for the analysis of rings in the vicinity of three-dimensional aromatic carboranes [30], and it is easily realised that the pitfalls warning applies to species that exhibit Möbius aromaticity as well. Indeed, it has been recommended that the observation of a NICS value that suggests aromaticity (or antiaromaticity) must be combined with an MICD plot to determine if the NICS value stems from a diatropic (or paratropic) ring current in the particular ring or if it is caused by other features in the current density [22]. In short, a negative (positive) NICS value is a necessary condition

for magnetic aromaticity (antiaromaticity), but it is not a sufficient condition.

At this point, it should be realised that essentially every aromaticity descriptor, not only NICS, has its specific limitations and pitfalls. For instance, the harmonic oscillator model of aromaticity (HOMA) gives a value of −5.93 for cyclobutane when based on the electron diffraction structure [31], and thus, this molecule would seemingly be more antiaromatic than cyclobutadiene (CBD) with a HOMA of −2.81 when based on the CASPT2/cc-pVDZ structure [32]. But cyclobutane is obviously not an antiaromatic molecule, and by (incorrectly) using HOMA on this molecule we are outside the set of compounds to which this descriptor can be applied. Similarly, the multicentre index (MCI), which describes the extent of electron delocalisation in a ring, gives an exactly zero value for two infinitely separated acetylene molecules as there is nil electron delocalisation between them. However, it gives a value of 0.010 for CBD (see the Supporting Information). Although MCI values of ~0 may indicate antiaromaticity, this does not mean that CBD is less antiaromatic than two separated acetylenes. Instead, it illustrates that two acetylenes are outside the set of molecular systems to which MCI can be applied as an (anti)aromaticity indicator. Similar considerations can be extended to nearly all aromaticity descriptors and highlight that the limitations, complications and pitfalls of various methodologies should be stressed more comprehensively in the literature in order to avoid improper use of the descriptors leading to incorrect (anti)aromaticity assessments. It also clarifies why several different types of aromaticity descriptors must be used in proper investigations of the potential (anti)aromaticity of new compounds [13–15]. Indeed, the search and identification of the various pitfalls and limitations can provide us with an improved overall understanding of (anti)aromaticity effects.

As is apparent, NICS values calculated in excited states can also falsely indicate excited-state Baird-aromatic character of a nonaromatic moiety when a neighbouring ring becomes Baird-antiaromatic. However, is this effect larger or smaller in the excited states than in the S_0 state? Or is there instead a difference between diatropic and paratropic ring currents in their abilities to generate NICS values that falsely suggest 'antiaromaticity' and 'aromaticity'? How general is the effect; does it apply to all $4n\pi$-cycles and to all $(4n+2)\pi$-cycles, or does it vary with the number of π-electrons in the cycle? In order to answer these questions, we explored compounds in which a nonaromatic ring in the form of a partially saturated ring, is situated next to two truly aromatic or antiaromatic rings (the nonaromatic ring can also be of another type, for example, the middle hexagon of perylene (Figure 1B) or a cross-conjugated ring). We then followed the changes in the false 'antiaromaticity' or 'aromaticity' upon excitation of the molecule as given by NICS and compared to changes in the MICD plots as well as the values from two electronic indices (MCI and FLU) and one geometric (HOMA) used as numerical anchors of nonaromatic character. It may be that NICS results for molecules in excited states are more likely to be misinterpreted as the energies of virtual transitions in the excited state are lower than in the ground state, which will result in stronger MICDs and larger NICS values [33]. The HOMA, FLU and MCI indices and the MICD plots were also used to describe the Hückel/Baird-(anti)aromatic character of the rings that exocyclically influence NICS values of these nonaromatic rings.

Although the pitfall of NICS analysed herein is known [23, 27–30], the foremost objectives of this study are to (i) explore and determine its relative impact in the assessment of (anti)aromatic character in excited states as compared with that in the S_0 state, and (ii) issue a pitfalls warning that helps curb incorrect usages of the NICS index in a hopefully pedagogical way. The findings reported serve as a set of examples on the risks when NICS is either the sole aromaticity indicator used to analyse new molecules, or when NICS values are overemphasised relative to values from other indices that give different answers. The results should help curb misunderstandings and incorrect assessments of (anti)aromatic character in both ground and excited states.

2 | Computational Methods

Geometry optimisations with enforced planarity were performed with Gaussian 16 [34], and single-point energy calculations for benchmarking were done with ORCA 6.0 [35]. We found that (U)B3LYP/6-311+G(d,p) geometries [36] lead to the lowest absolute energies in DLNPO-(U)CCSD(T)//(U)DFT computations and give qualitatively the same results as other methods (see section S1.1 in Supporting information for further details). The optimised planar geometries are not always minima, but saddle points between nonplanar conformers. We studied these structures to maximise the (de)shielding effects of the π-systems in the molecules.

The following (anti)aromaticity indicators were used to investigate the molecules: $NICS(0)_{\pi zz}$, $NICS(1)_{\pi zz}$, NICS-*XY* scans [19, 37–39], NICS to bond current (NICS2BC) [23], anisotropy of induced current density (ACID) [40], MICD [41], fluctuation index of aromaticity (FLU) [42], MCI [43], HOMA [44], and harmonic oscillator model of excited-state aromaticity (HOMER) [32]. CASSCF $NICS(1)_{zz}$ and $NICS(1.7)_{zz}$ calculations were performed for monocycles in their S_0, T_1 and S_1 states with Dalton 2016 [45].

The use of NICS scan methods is recommended for polycyclic (anti)aromatic molecules, and the use of $NICS(1)_{\pi zz}$ is suggested for monocycles [39, 46]. The use of the NICS(0) approach is not recommended as the electron densities affect its results, but such results are still published in the literature [47]. Herein, we only used this technique to highlight its errors. $NICS(1.7)_{zz}$ results below −5 ppm indicate aromaticity, above 5 ppm suggest antiaromaticity and between −5 and 5 ppm correspond to nonaromatic character [39]. Although these ranges are only suggested for the $NICS(1.7)_{zz}$ values, we used them as references for other NICS methods as well. HOMA indicates aromaticity when values are in the range 0.5–1.0, while lower values reveal nonaromatic or antiaromatic character [44]. The FLU and MCI are electronic aromaticity descriptors that reflect the extent of electron sharing between atoms. A FLU value close to 0 for a ring signals aromaticity, while larger values indicate nonaromatic cycles [42]. An MCI value close to 0.07 in 6-membered rings (6-MRs) indicate aromaticity and values close to 0 correspond to nonaromatic or antiaromatic moieties [43]. A drawback of these non-magnetic indices is, however, that they cannot separate antiaromaticity from nonaromaticity as such values are similar.

3 | Results and Discussion

Here, we present results on molecules where two properly aromatic or antiaromatic moieties (rings *a* and *a′*) are separated by a partially saturated ring (ring *b*) having at least two methylene moieties (Figure 2). Thereby, we ensure that there is no hyperconjugative aromaticity of the type that can be found in cyclopentadiene derivatives (see S1.7 in Supporting information) [48]. The molecules were studied in enforced planar structures in order to achieve maximal deshielding or shielding effects by the ring currents in, respectively, the aromatic or antiaromatic rings. The nonaromatic middle ring (ring *b*) was flanked by either two aromatic or two antiaromatic rings *a* and *a′* so as to reinforce the deshielding or shielding effect. We considered two cases where the rings *a* and *a′* either interact or are fully separated. First, we analyse the results of 9,10-dihydrophenanthrene (**1**), a compound with two interacting Hückel-aromatic benzene rings in its S_0 state, and two interacting potentially Baird-antiaromatic rings in its first quintet state (Q_1). We then compare **1** with compounds **2**–**5**, which in their T_1 or Q_1 states are Baird-aromatic analogues of **1** in its Hückel-aromatic S_0 state. This comparison should shed light on the extent of deshielding in ring *b* as induced by the Hückel-aromaticity in S_0 as compared to the Baird-aromaticity in the excited state of rings *a* and *a′*.

In order to analyse the effect of the connectivity, the saturated ethylene bridge was exchanged to two saturated methylene bridges, resulting in 9,10-dihydroanthracene (**6**) and its analogues **7**–**10** where the two annulene rings are non-interacting. This elucidates the generality of the influence of aromatic moieties on the NICS of adjacent nonaromatic rings. We further replaced the middle cyclohexa-1,3-diene ring with cycloocta-1,4-diene (**11**–**13**) in order to study the distance dependence of the influence of the shielding and deshielding effects. Although we mainly discuss computed results on species in their lowest polyradicaloid triplet and quintet ππ* states, towards the end we also explore NICS scans of the lowest singlet excited ππ* states (S_1) of benzene and cyclooctatetraene, and compare with those in the T_1 and S_0 states. While further analogous compounds can be drawn, this set of molecules reveals the various aspects of the pitfalls with (anti)aromaticity analyses primarily based on NICS.

In Section 1, we described a pitfall of NICS that can lead to misinterpretations if ignored, that is, if NICS is used incorrectly. As stated above, other aromaticity descriptors also have pitfalls and can be used incorrectly. However, there are differences. First, NICS is used to assess molecules that range from aromatic to antiaromatic, while HOMA, FLU and MCI are mainly used to separate aromatic cycles from non/antiaromatic ones. Another difference between NICS versus HOMA, FLU and MCI is that the magnetically induced current density, which NICS reflects, creates (de)shieldings in both the interior and exterior of an (anti)aromatic cycle whereas the effects of HOMA, FLU and MCI are more spatially confined to a particular ring. As a result, the HOMA, FLU and MCI indices should give results that only depend on the middle ring *b* and they should not differ extensively by the (anti)aromatic character of the side rings *a* and *a′* (see S1.5 in Supporting information). Hence, the values of these indices for the nonaromatic ring *b* should be essentially the same in ground and excited states. For that reason, we utilise HOMA, FLU and MCI as numerical anchors for the lack of aromaticity of ring *b*. On the other hand, for rings *a* and *a'* the three indices as regular reflect the aromatic vs. non/antiaromatic character in the molecules of the various electronic states.

3.1 | 9,10-Dihydrophenantrene

The two connected benzene rings in 9,10-dihydrophenanthrene (**1**) can be seen as a biphenyl molecule constrained by a saturated ethylene (—CH_2CH_2—) bridge (Figure 2). Biphenyl in its S_0 state is known to have a long inter-ring CC bond (1.507 Å) and a slightly twisted structure [49]. However, in its T_1 and S_1 states, there is a π-interaction between the two benzene rings, resulting in planar structures with shorter inter-ring CC bonds (~1.41 Å) [50, 51]. Biphenyl has not been explored in its Q_1 state, yet, we hypothesise that **1** in its Q_1 state will become doubly Baird-antiaromatic with two triplet-state Baird-antiaromatic benzene rings *a* and *a′*. Ring *b*, on the other hand, should be nonaromatic in both states. However, for the latter ring we hypothesise that NICS will indicate antiaromaticity in S_0 and aromaticity in Q_1, while the other indicators (HOMA, FLU and MCI) will give similar results in the two states, that is, suggest nonaromatic character in both states. Furthermore, according to our hypothesis,

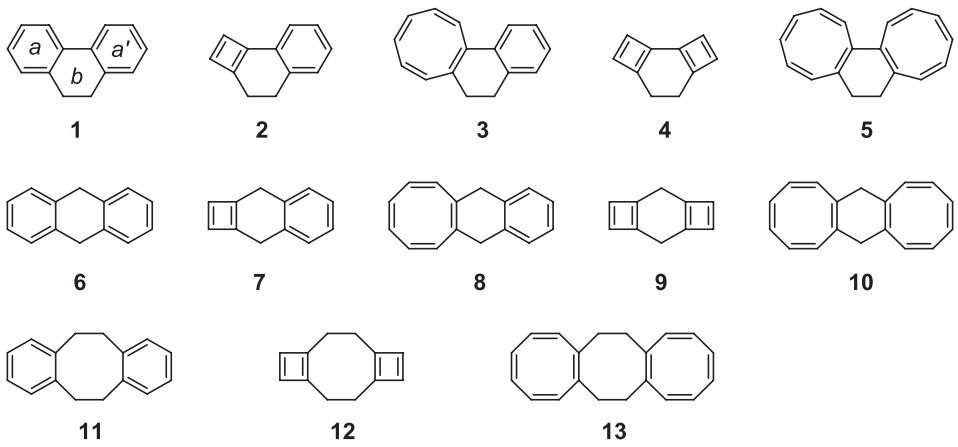

FIGURE 2 | Investigated compounds **1**–**13** with the nonaromatic middle rings *b* for which NICS falsely suggests as having 'aromatic' or 'antiaromatic' character to various extents. Rings *a*, *b* and *a′* are shown for **1**.

the MICD maps, which the NICS values reflect, should not exhibit any ring currents over ring *b* in either state.

Interestingly, the two benzene rings in the planar structure of the Q_1 state are not equivalent because a C_s symmetric structure with only enforced planarity is 12.5 kcal/mol lower in energy than a C_{2v} symmetric structure described by two equally Baird-antiaromatic benzene rings represented as two *bis*(allyl) triplet diradicals. Our computations indicate that the C_s symmetric Q_1 state should be described as a combination of one allyl radical, one trimethylene methane diradical and one pentadienyl radical (Figure 3). This finding is in line with simple Hückel molecular orbital theory because the latter description is lower in energy by 0.43 β than that of four allyl radicals (see S1.4 in Supporting information) [52]. The lowered symmetry of the Q_1 state can also be seen in the NICS results as the two benzene rings have slightly different values, yet, they still reveal strong Baird-antiaromaticity (Figure 3). Hence, the two benzene rings interact in Q_1, but not to the extent that the antiaromaticity is alleviated. The inter-ring CC distance is shortened from 1.488 Å in S_0 to 1.386 Å in Q_1.

Indeed, based on our computed $NICS(0)_{\pi zz}$ and $NICS(1)_{\pi zz}$ values in S_0 (Figure 3A), ring *b* would be categorised as weakly 'antiaromatic'. The NICS data further show that ring *b* of **1** goes from 'antiaromatic' in S_0 to 'aromatic' in Q_1 (in S_0 $NICS(1)_{\pi zz} = 8$ ppm while in Q_1 $NICS(1)_{\pi zz} = -11$ ppm, Figure 3A), confirming our hypothesis. However, NICS scans (NICS-*XY*) are often more suitable for polycyclic molecules than individual NICS values computed at ring centres [38, 39]. Still, the patterns from individual NICS values are also apparent when the two states are examined through NICS-*XY* scans as these scans reflect deshieldings over ring *b* in S_0 and shieldings in Q_1 (Figure 3B). Here, it should be noted that NICS values of antiaromatic rings generally are larger in magnitude than those of aromatic ones as a result of energies of the virtual transitions involved [33]. Thus, as the NICS value of ring *b* is smaller in magnitude than those of the properly Hückel-aromatic rings *a* and *a′* in S_0 (Figure 3), one may dismiss the false 'antiaromaticity' of ring *b* in S_0. However, the false 'aromaticity' of ring *b* of **1** in the Q_1 state cannot be dismissed by such an argumentation as the relationship in the magnitudes of NICS values in rings *a* and *a′* vs. *b* is opposite to that in S_0.

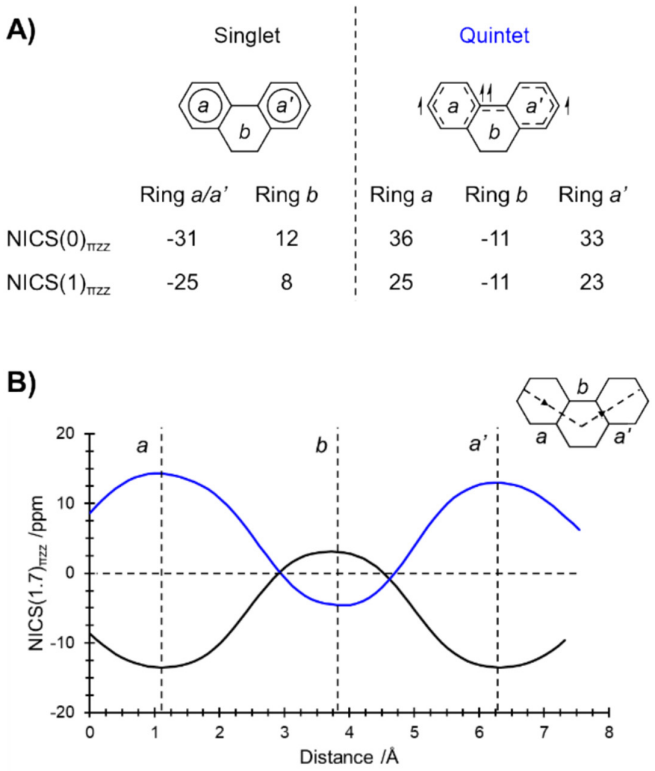

FIGURE 3 | NICS analysis of molecule **1**. (A) NICS values for the three rings of **1** and (B) NICS-*XY* scans above molecule **1** in S_0 (black line) and Q_1 (blue line) states. All NICS values are given in ppm and calculated at GIAO-(U)B3LYP/6-311+G(d,p)//(U)B3LYP/6-311+G(d,p) level.

Now, to resolve if NICS falsely indicates '(anti)aromatic' character for ring *b*, we view the MICD maps of both states as well as the changes in the numerical values in the nonmagnetic HOMA, FLU and MCI indices when going from S_0 to Q_1 (Figure 4 and Table 1). Yet, we first consider the 'Baird-aromatic' character of ring *b* in the Q_1 state by looking at the spin density. Baird-aromaticity is represented by extensive spin delocalisation leading to a nearly uniform excess of α-spin density over a cycle [53]. This is the case in the Baird-aromatic T_1 states of CBD and cyclooctatetraene (COT) [53]. However, no uniform spin delocalisation can be observed over ring *b* in the Q_1 state of **1** (Figure 4A), ruling out any Baird-type aromatic character of this ring. Instead, the shielding (reflected by NICS) is a consequence of the magnetically induced ring currents in the two neighbouring rings *a* and *a′*, not in ring *b* itself. In the Q_1 state, as well as the S_0 state, the MICD maps of **1** do not show any current densities along the single bonds of the *b* ring, while proper ring currents can be seen in the benzene moieties in both states (Figure 4B,C). This highlights the importance of critically scrutinising preliminary conclusions based on NICS against the actual current density of computed MICD plots [22].

The geometric and electronic (anti)aromaticity aspects as given by HOMA, FLU and MCI were also considered and compared between the states of **1** (Table 1, for information on the numerical ranges of these indicators see the Computational Methods section). Importantly, these indicators cannot be used to assess any (anti)aromatic character of (partially) saturated rings as described above. Yet, as they act more locally than NICS, we use them as numerical anchors whereby they should remain essentially unaffected by the change in (anti)aromatic character of the neighbouring rings *a* and *a′* that occurs upon electronic excitation of **1**. Now, with regard to rings *a* and *a′*, all indices (HOMA, FLU, MCI and NICS) reveal substantial changes when **1** goes from S_0 to Q_1, and importantly, the various values of these rings resemble those of our reference compound, benzene in S_0 and T_1 (Table 1). However, in contrast to NICS, neither index shows any essential differences in their numerical values for ring *b* when going from S_0 to Q_1 (Table 1).

Molecule **1** was also investigated in its T_1 and S_1 states, and we found that it retains its C_{2v} symmetry when constrained to planarity, similar as in the S_0 state, and that the structures in T_1 and S_1 are very similar. Although these planar structures are transition states (the minima are twisted), the parent

biphenyl molecule, as mentioned above, has planar T_1 and S_1 structures [50]. This means that the π-system in molecule **1** prefers planarity in the excited states, but the steric interactions in the eclipsed conformation of the ethylene moiety of ring *b* counteracts it. The increased π-interaction can also be seen in the shortening of the inter-ring CC bond from 1.488 Å in S_0 to 1.388 Å in T_1 and to 1.417 Å in S_1. However, in its T_1 state, the benzene rings of **1** are computed to be nonaromatic (for further details, see S1.3.1 in Supporting information).

Taken together, these computational results reveal that the known pitfall of false 'antiaromatic' NICS values that appear in rings adjacent to localised (Hückel-aromatic) diatropic ring currents [23] can be extended to excited-state (Baird-antiaromatic) paratropic ring currents, and in the latter case NICS falsely indicates 'aromaticity'. In order to probe the effect of excited-state aromatic rings, we next replaced one or both benzene rings in **1** with triplet state Baird-aromatic CBD and COT rings [15, 54], giving compounds **2**–**5** (Figure 2).

3.2 | Excited-State Aromatic Analogues of 9,10-Dihydrophenanthrene

For the excited-state aromatic species **2**–**5**, we probe if the extent of false 'antiaromaticity' of the nonaromatic ring *b* (as given by NICS) can be larger when caused by Baird-aromatic 4*n*π-electron cycles than when caused by the Hückel-aromatic benzene rings of compound **1** in S_0 (Figure 5). Hence, **2**–**5** were computed in their Baird-aromatic ππ* excited states, which means T_1 states for **2** and **3** as only one 4*n*π-electron ring can be Baird-aromatic in them, while **4** and **5** were studied in their Q_1 states as they contain two 4*n*π-electron rings that both can be Baird-aromatic.

As noted above, a first indicator for triplet state Baird-aromaticity is the spin density [53]. In the case of a Baird-aromatic cycle, there must be a uniformly distributed excess of α-spin over the complete cycle. Based on our calculations, the excess of α-spin density in **2**–**5** are distributed evenly over the CBD and COT rings (Figure 5B), in line with Baird-aromatic character. The benzene rings of **2** and **3**, on the other hand, exhibits alternating excess of α- and β-spin densities, indicative of spin polarisation and only little excess of α-spin density. This suggests that the benzene ring is Hückel-aromatic.

A proper assessment of the extent of Baird- and Hückel-aromatic character of the two rings in **2** and **3** can be achieved via the ΔFLU/FLU values, where ΔFLU is the difference between FLU_α and FLU_β. The ΔFLU/FLU value differentiates Hückel-aromatic cycles ($FLU_\alpha = FLU_\beta$), with (near-)zero ΔFLU/FLU values, from Baird-aromatic ones ($FLU_\alpha \neq FLU_\beta$) with nonzero ΔFLU/FLU values close to that of a suitable fully Baird-aromatic reference molecule [17]. In the T_1 state of **3**, ring *a* (the COT ring) has a ΔFLU/FLU of 1.60, whereas in ^{3}COT, used as reference, it is 2.73. The benzene ring in **3** (ring *a*′) has a value of 0.33, which is rather close to that of benzene in S_0, the Hückel-aromatic reference, with a value of exactly

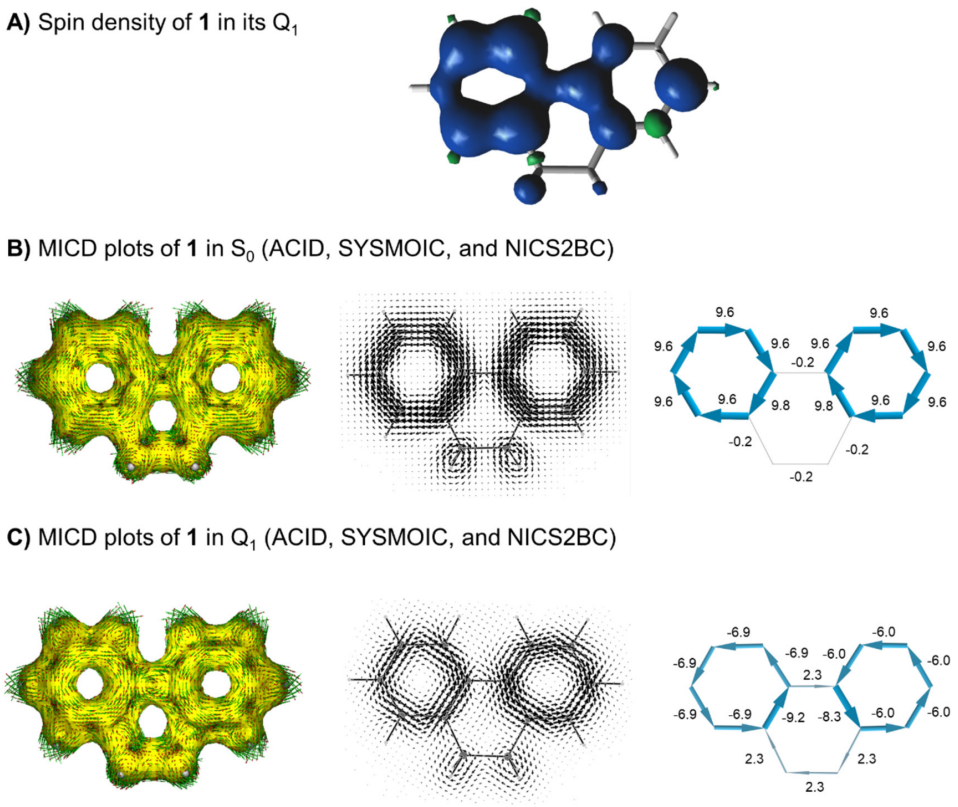

FIGURE 4 | Spin density of **1** in Q_1 and magnetically induced current densities of **1** in its S_0 and Q_1 states. (A) Spin density plot calculated at UB3LYP/6-311+G(d,p) level (isovalue 0.004 a.u.); (B) Magnetically induced ring current density plots of **1** in its S_0 state visualised with ACID (GIAO-B3LYP/6-311+G(d,p), isovalue 0.025 a.u.), SYSMOIC (CSGT-B3LYP/6-311+G(d,p)) and NICS2BC (GIAO-B3LYP/6-311+G(d,p)); (C) MICD plots of **1** the in Q_1 state with ACID, SYSMOIC and NICS2BC. The plots generated by SYSMOIC were only containing the π- orbital contributions to the MICDs.

TABLE 1 | HOMA, FLU and MCI values of **1** in its S_0 and Q_1 states and benzene (used as 6-MR reference) in its S_0 and T_1 states.

Aromaticity index	Molecule (state)	Ring *a*	Ring *b*	Ring *a′*
HOMA	Benzene (S_0)	0.990 [a]	—	—
	Benzene (T_1)[b]	−0.491[a]	—	—
	1 (S_0)	0.963	(*−1.894*)[c]	0.963
	1 (Q_1)	−0.329	(*−1.538*)[c]	0.157
FLU	Benzene (S_0)	0.000[a]	—	—
	Benzene (T_1)[b]	0.024[a]	—	—
	1 (S_0)	0.001	(*0.055*)[c]	0.001
	1 (Q_1)	0.034	(*0.055*)[c]	0.026
MCI	Benzene (S_0)	0.072[a]	—	—
	Benzene (T_1)[b]	0.000[a]	—	—
	1 (S_0)	0.061	(*0.001*)[c]	0.061
	1 (Q_1)	0.007	(*0.001*)[c]	0.010

Note: Calculated with (U)B3LYP/6-311+G(d,p).
[a]Calculated for the benzene ring.
[b]Calculated for the *bis*(allyl) triplet benzene bond-shift isomer.
[c]Italicised values in parentheses do not indicate aromaticity or antiaromaticity as the HOMA, FLU and MCI indices are applied outside their respective limitations.

zero. These two values of **3** support significant Baird-aromatic character of the COT ring and Hückel-aromatic character of the benzene ring, but there is also some spin delocalisation from the COT ring to the benzene ring.

Based on various aromaticity indicators described above, the $4n\pi$-electron cycles *a* and *a′* of **2**–**5** gain aromatic character in the investigated high-spin states (see S1.3.2–S1.3.5 in the Supporting information). The diatropic ring currents in these rings induce positive NICS values for the nonaromatic ring *b* (Figure 5C), similar as for **1** in S_0. However, no proper ring currents form in ring *b* as seen in the MICD plots of the molecules (for **3** see Figure 5D, for **2**, **4** and **5** see S1.3 in Supporting information), while clear diatropic ring currents form in both rings *a* and *a′*. In rings *b*, only weak localised currents can be observed around the CH_2 moieties. Furthermore, the HOMA, FLU and MCI indices give essentially the same numerical values for the rings *b* of **2**–**5** in their T_1 or Q_1 state as for ring *b* of **1** in its S_0 state (see S1.5 in Supporting information). In contrast, as an example, the values in **3** indicate Hückel-aromaticity for ring *a* (HOMA: 0.924, FLU: 0.0020) and Baird-aromaticity for ring *a′* (HOMA: 0.859, FLU: 0.0031). Thus, if only NICS values were to be considered as the computational indicator of (anti)aromaticity, one would falsely conclude on weak 'antiaromatic' characters of ring *b* of **3** and **5**. On the other hand, as values below 5 ppm represent nonaromatic character [39], rings *b* in **2** and **4** would not be mislabelled. Interestingly, a comparison of the NICS values of rings *b* of **1** in S_0, **2** and **3** in T_1, and **4** and **5** in Q_1, reveals that the NICS value becomes the most positive, falsely indicating 'antiaromaticity', when caused by a Baird-aromatic ^{3}COT ring and the least positive when caused by a Baird-aromatic ^{3}CBD ring. A closed-shell Hückel-aromatic benzene ring has an intermediate influence.

3.3 | 9,10-Dihydroanthracene and Analogues

To investigate the exocyclic (de)shielding effect in species with two non-interacting rings *a* and *a′*, we replaced the middle cyclohexa-1,3-diene of **1**–**5** with a cyclohexa-1,4-diene unit, resulting in 9,10-dihydroantracene (**6**) and analogous molecules **7**–**10**. The middle cyclohexa-1,4-diene ring was further replaced by a cycloocta-1,5-diene ring, leading to **11**–**13**, allowing us to determine the distance dependence of the shielding and deshielding effects.

We first explored compounds **6**–**10** (Figure 6A) in their most aromatic states, whereby **7**–**10** were investigated in their Baird-aromatic high-spin $\pi\pi^*$ states. The (de)shielding effect reflected by the NICS values is shown for both the first (**1**–**5**, Figure 6B) and second (**6**–**10**, Figure 6C) set of molecules. A trend is apparent for both sets: the NICS value of ring *b* is not correlated with the NICS values of ring *a* and *a′* (see S1.6 in Supporting information) but mostly increases with the total number of π-electrons in the compounds, in line with earlier findings by Mills and Llagostera [55]. The exceptions are **5** and **10** with two COT rings, as they have smaller NICS values than **3** and **8** composed of one COT ring and one benzene ring. Thus, it is noteworthy that contrary to our expectation, the (de)shielding effect does not depend on the Hückel- vs. Baird-aromatic nature of the aromaticity. Furthermore, if we compare the individual compounds among **1**–**5** with the corresponding analogues of **6**–**10**, we see that the deshielding effect by rings *a* and *a′* on ring *b*, reflected via the NICS values, is always lower in the second set of compounds where the two rings do not interact.

Finally, in **4** and **9** that have two CBD rings, the exocyclic deshielding effect is negligible, and compound **9** in Q_1 even has a negative NICS value indicating no influence from the π-system. The source of the negative value could be the σ-skeleton as cyclohexane has a NICS value of −2.2 ppm in the middle of its ring [19], similar to that of **9** in Q_1. Here, the MICD maps of the molecules resolve the false 'antiaromaticity' suggested by NICS in **6**–**8** and **10** as no proper paratropic ring current can be seen in ring *b*, only localised circulations in the current density (for **4** and **9** see Figure 6D, for the other molecules see S1.3 in Supporting information). Furthermore, looking at MCI, FLU and HOMA we observe no significant differences in these values among the investigated molecules (for the values of **6**–**10** see S1.5 in Supporting information, for the values of **6**, **9** and **10** see also Table 2).

The distance dependence of the exocyclic (de)shielding, via the NICS values, was explored through the comparison of (i) molecules **6** and **11** in their doubly Hückel-aromatic S_0 states and in their doubly Baird-antiaromatic Q_1 states and (ii) molecules **9**, **10**, **12** and **13** in their doubly Hückel-antiaromatic S_0 states and in their doubly Baird-aromatic Q_1 states (Figure 7). First of all, the HOMA, FLU and MCI values reflect a nonaromatic character of rings *b* in these compounds because the respective values

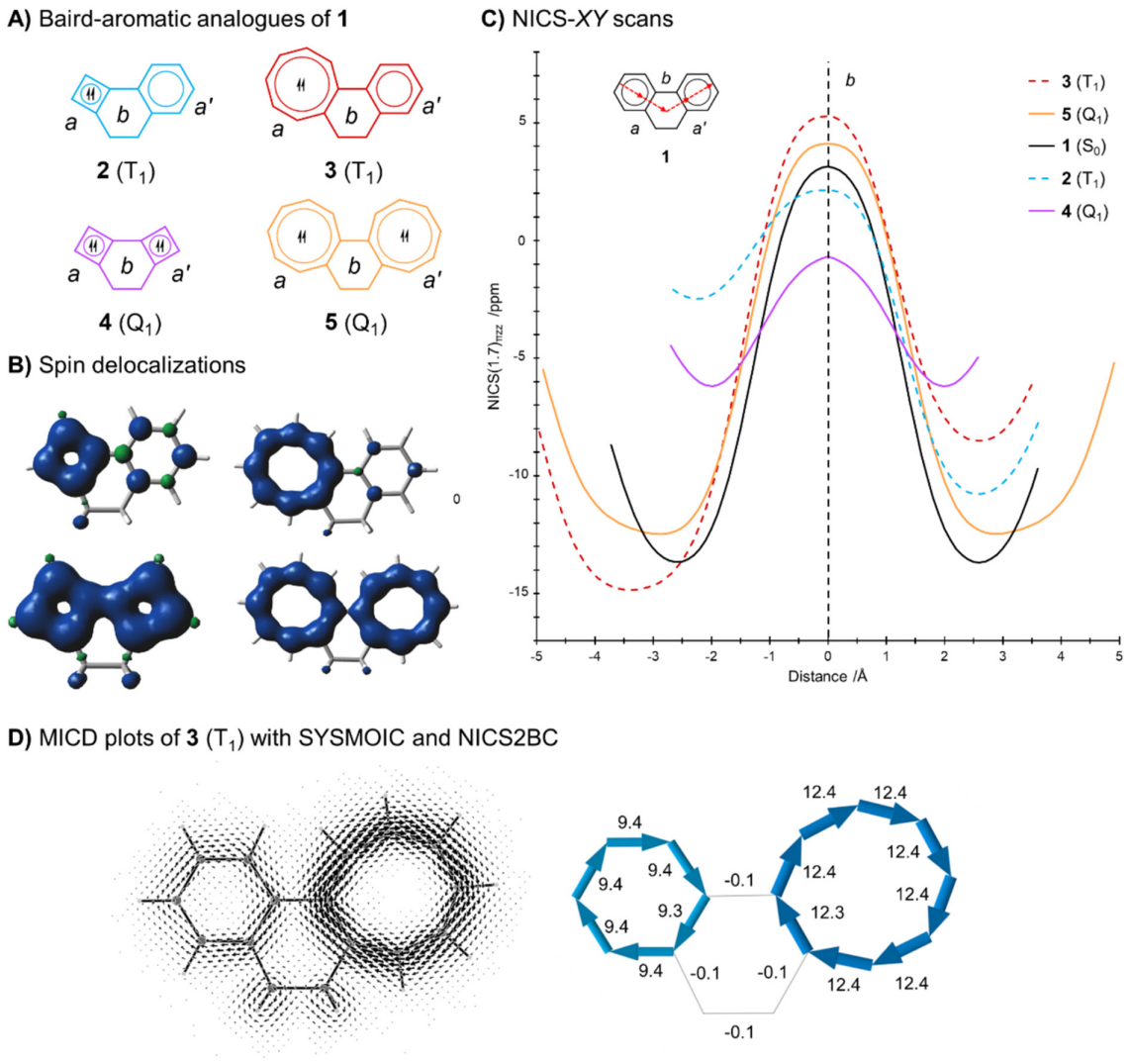

FIGURE 5 | Aromaticity assessment of the Baird-aromatic **2**–**5** compounds. (A) Excited-state Baird-aromatic analogues **2**–**5** of molecule **1**. (B) Spin density plots calculated at UB3LYP/6-311+G(d,p) level (isovalue 0.004 a.u.). (C) NICS-*XY* scan NICS(1.7)$_{\pi zz}$ values vs. distance from the middle of *b* ring (solid lines correspond to symmetric and dashed lines correspond to asymmetric molecules in their aromatic ground or excited states), and (D) magnetically induced current density plots of **3** in its T_1 state.

do not change for this ring between molecules with the same type of ring and between the electronic states (Table 2). The values for ring *b* are almost independent of the (anti)aromatic character of the side rings *a* and *a′* (see Table S19 in the Supporting information). The changes in MCI are nil while modest changes occur in the HOMA and FLU values due to bond order changes in the common bonds of ring *b* with rings *a* and *a′*. Despite this, they still do not suggest a switch in the (anti)aromatic character of the middle ring, in stark contrast to NICS.

With regard to the COT ring, it is first notable that its (de)shielding effect on ring *b* measured by NICS is largest both in the doubly diatropic (aromatic) Q_1 states of **10** and **13** and in the doubly paratropic (antiaromatic) S_0 states of these two compounds (Figure 7). It is further noteworthy that the shielding effect of the paratropic COT rings *a* and *a′* on the NICS values of ring *b* in S_0 is larger than the deshielding effect of the diatropic ^{3}COT rings *a* and *a′* in Q_1, and that this is valid for both **10** and **13**. Conversely, the weak exocyclic deshielding of the ^{3}CBD ring is seen via compounds **9** and **12** in their Q_1 states as they show no changes with distance and even lead to a negative NICS value, despite that both ^{3}CBD rings are Baird-aromatic. This feature should have produced positive NICS values in ring *b*.

Through these comparisons we can observe three major trends on the influence of NICS values in ring *b*: (i) first, the influence of COT rings (as *a* and *a′*) on the NICS value of ring *b* is the largest while CBD rings give the smallest, (ii) secondly, the influence of antiaromatic rings (as *a* and *a′*) is larger than that of aromatic ones, and (iii) finally, as can be expected, the influence is attenuated with distance from the induced ring current.

3.4 | Extension to the Lowest Singlet Excited State

We showed that the (de)shielding influence by neighbouring rings can lead to misinterpretations on the (anti)aromatic

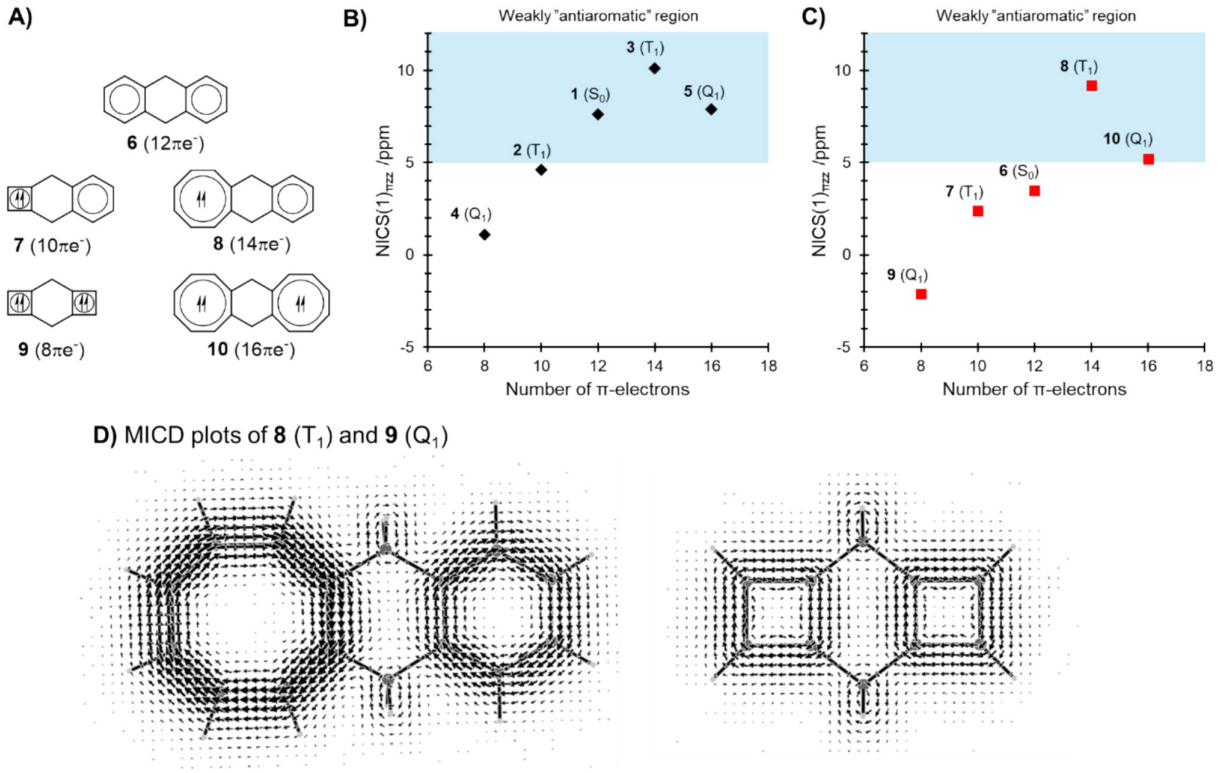

FIGURE 6 | Investigation of 9,10-dihydroantracene and its analogues (**6**–**10**), comparisons of the effects of $4n\pi$-moieties, and the distance dependence in S_0 and Q_1 states. (A) 9,10-dihydroantracene and its analogues; (B) $NICS(1)_{\pi zz}$ values above the nonaromatic ring *b* vs. the number of π-electrons in **1**–**5**; (C) $NICS(1)_{\pi zz}$ values above the middle nonaromatic ring *b* vs. the number of π-electrons in **6**–**10**. Points in the blue regions would be falsely labelled as 'antiaromatic' based on NICS. (D) Magnetically induced current density plots of **8** in its T_1 and **9** in Q_1 states.

character of nonaromatic rings in the S_0 state and also in the lowest triplet and quintet excited states. This triggered us to look at the exocyclic (de)shielding influence of benzene and COT in their first singlet excited state (S_1), which is the state where most photochemical transformations occur. The CBD ring was not considered as its influence was the smallest among the conjugated cycles studied.

The complete active-space self-consistent field (CASSCF) wave functions, constructed from gauge-including atomic orbitals (GIAOs), was used to obtain the shielding tensors for these molecules. The S_1 structures were calculated at TD-B3LYP/6-311+G(d,p) level. The $NICS(1)_{zz}$-*XY* scans from the middle of the ring outwards above a bond for benzene were calculated at CASSCF(6,6)-GIAO/6-31++G(d,p) and for COT at CASSCF(8,8)-GIAO/6-31++G(d,p) levels (Figure 8) [56]. Because we changed the methodology from DFT to CASSCF we also calculated NICS for the S_0 and T_1 states of benzene and COT at the latter level.

It is known that there are three nearly isoenergetic isomers of benzene in its T_1 state. Two of them are planar bond-shift isomers [57]. We refer to them as *bis*(allyl) and quinoid. We explored both and found that the results are similar (blue and green benzene results in Figure 8). In the structures where the CC bonds are inequivalent, that is, in D_{2h} and D_{4h} symmetric ones, we also note above which bond the scan is run. Yet, we found that the NICS results are both qualitatively and quantitatively similar in such cases.

TABLE 2 | HOMA, FLU and MCI values of ring *b* in compounds **6** and **9**–**13** in their S_0 and Q_1 states.

Molecule	State	HOMA	FLU	MCI
6	S_0	−1.664	0.057	0.001
6	Q_1	−1.188	0.053	0.001
9	S_0	−1.265	0.069	0.001
9	Q_1	−1.218	0.059	0.001
10	S_0	−1.908	0.069	0.001
10	Q_1	−2.153	0.059	0.001
11	S_0	−3.610	0.067	0.000
11	Q_1	−2.799	0.069	0.000
12	S_0	−3.979	0.071	0.000
12	Q_1	−2.371	0.063	0.000
13	S_0	−3.906	0.077	0.000
13	Q_1	−4.633	0.070	0.000

Note: Calculated with (U)B3LYP/6-311+G(d,p).

Based on our results, benzene in its S_1 state is more antiaromatic than in its T_1 state, while the COT is qualitatively at the same level of aromaticity in its lowest two excited states, in line with studies by Karadakov and co-workers [10]. And this difference between the excited-state antiaromaticity of benzene in its S_1

and T_1 states can also be seen in the exocyclic influence on the shielding, as it is larger in S_1 than in T_1.

The NICS(1)$_{zz}$ scans of benzene and COT in all states show that the influence of the shielding at the distance where the centre of a virtual annelated hexagon would have been placed (red dotted line in Figure 8) is as expected, that is, there is a deshielding on the outside of aromatic rings and shielding on the outside of antiaromatic one. However, in these NICS-*XY* scans (Figure 8), one can see the influence of the σ-skeleton (the dips next to the red dashed lines). To eliminate this influence, we also performed the scans at 1.7 Å (see S1.8 in Supporting information) and found that the influence decreases significantly with the height; NICS(1.7)$_{zz}$ indicates aromaticity on the outside of the rings, which looks slightly stronger next to antiaromatic rings.

Taken together, these findings extend the number of examples where NICS incorrectly indicate (anti)aromaticity in subunits of complex molecules, not only in ground states [23, 27, 30] but also in excited states [28].

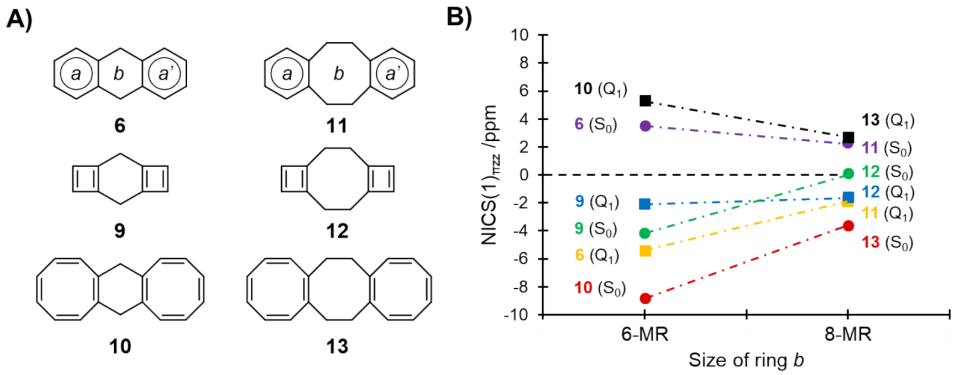

FIGURE 7 | Distance dependence of aromatic and antiaromatic rings influence on the neighbouring ring *b*. (A) The investigated molecules and (B) NICS(1)$_{\pi zz}$ values above ring *b* of the molecules in their S_0 (circle) and Q_1 (square) states. The connected points correspond to molecules with common side rings in the same states but with different rings *b*.

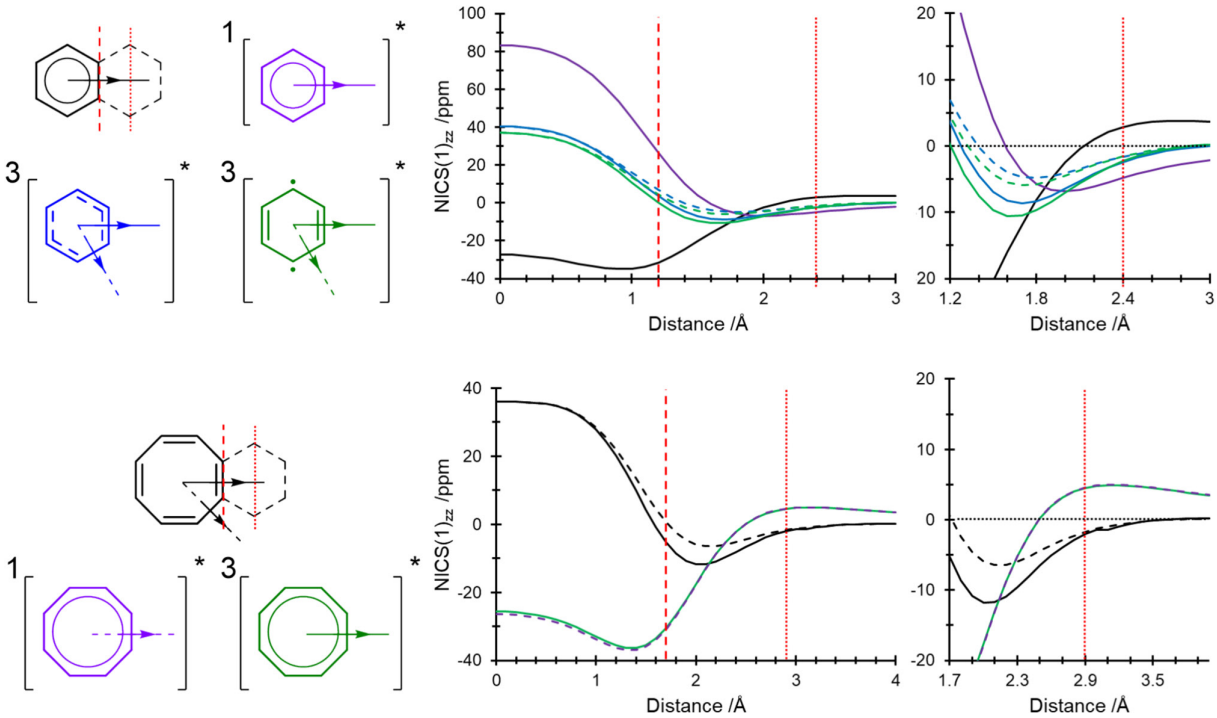

FIGURE 8 | NICS(1)$_{zz}$-*XY* scan at S_0, S_1 and T_1 states above benzene and COT calculated at CASSCF(6,6)-GIAO/6-31++G(d,p) level and CASSCF(8,8)-GIAO/6-31++G(d,p) level of theory, respectively. In the middle column, the full scans from the middle to 3 Å and 4 Å distances for benzene and COT, respectively; in the right column, the exocyclic region of the scan. The top line contains the data for benzene, and the bottom one contains it for COT. The red dashed line represents the point where the scan crosses the bond, and the red dotted line represents the distance where the middle of an annelated hexagon would be located. The black line corresponds to the ground state results; the purple colour corresponds to the S_1 state of molecules; the green and blue lines correspond to the T_1 state of molecules.

4 | Conclusions

In this work, we explored the influence of ground state (Hückel) and local triplet excited-state (Baird) (anti)aromatic rings on the NICS values of neighbouring nonaromatic rings which are partially saturated with either one saturated ethylene ($-CH_2CH_2-$) segment or two methylene ($-CH_2-$) segments. We found that these nonaromatic rings exhibit NICS values that generally correspond to weakly aromatic or antiaromatic cycles. However, these are false 'aromaticity' or 'antiaromaticity' indications as these rings have several saturated carbon atoms. Instead, exocyclic shielding and deshielding effects from the magnetically induced ring currents of neighbouring rings are the sources of these NICS values. These partially saturated middle rings exhibited no proper magnetically induced ring currents and the values of the electronic and geometric descriptors do not change upon excitation indicating nonaromatic character in them. Combined, it becomes apparent that NICS can be misinterpreted to indicate 'aromatic' or 'antiaromatic' character, and that (anti)aromaticity assessments with NICS should be supported by plots of magnetically induced current densities and/or results from other (anti)aromaticity descriptors.

The relative influence of Hückel- vs. Baird-aromatic as well as antiaromatic cycles on the NICS values was also investigated. No indication of a general increase or a general decrease in the magnitude of the exocyclic (de)shielding effect due to excited-state aromaticity was found. However, if one compares the Hückel-aromatic state to the Baird-antiaromatic state of a molecule, one finds that antiaromatic rings have greater (de)shielding influence than aromatic ones. Interestingly, this is also true when we compare Hückel-antiaromatic to Baird-aromatic states. In general, the exocyclic influence by antiaromatic cycles is greater than that by aromatic ones, and consequently, it is more common to encounter false 'aromaticity' than false 'antiaromaticity' based on NICS results.

The effect of the number of π-electrons in the aromatic ring was also considered, and it was observed that the CBD rings have the smallest influence, benzene rings are intermediate, and COT rings have the largest influence on exocyclic (de)shielding and NICS. The distance dependence of the influence was explored by comparing results for 6-MR and 8-MR cores. When going from central nonaromatic 6-MRs to 8-MRs, the magnitude of the NICS value decreases significantly, and it properly corresponds to no aromaticity or no antiaromaticity. Thus, the pitfalls warning is especially needed when assessing aromaticity in small (nonaromatic) rings next to large antiaromatic ones. The exocyclic relationship on the NICS values (i.e., false indication of 'antiaromaticity' next to aromatic rings and vice versa) was also applicable to the first singlet excited state, which is important for photochemical and photophysical processes.

All in all, we brought examples of simple molecules where the exocyclic (de)shielding effect of induced ring current in neighbouring (nonaromatic) rings on the NICS value is clearly identifiable. The findings illustrate the importance of a careful analysis of induced ring currents, and that overemphasis on computed NICS data can lead to misinterpretations.

Author Contributions

Péter J. Mayer: conceptualization, data curation, investigation, writing – original draft. **Henrik Ottosson:** conceptualization, funding acquisition, writing – review and editing, supervision.

Acknowledgements

First of all, we thank Dr. Ouissam El Bakouri for initial computations on this project. The Carl Trygger Foundation for a postdoctoral scholarship to P.J.M. (grant CTS 22: 2330) and the Swedish Research Council for financial support to H.O. (grant 2023-04179) are gratefully acknowledged. The computations were enabled by resources provided by the National Academic Infrastructure for Supercomputing in Sweden (NAISS), partially funded by the Swedish Research Council through grant agreement no. 2022-06725.

Data Availability Statement

The data that supports the findings of this study are available in the supplementary material of this article.

References

1. V. I. Minkin, M. N. Glukhovtsev, and B. Y. Simkin, *Aromaticity and Antiaromaticity: Electronic and Structural Aspects* (New York: Wiley, 1994).

2. P. v. R. Schleyer, "Introduction: Aromaticity," *Chemical Reviews* 101 (2001): 1115–1118.

3. I. Fernández, *Aromaticity: Modern Computational Methods and Applications* (Amsterdam: Elsevier, 2021).

4. M. Solà, A. I. Boldyrev, M. K. Cyrañski, T. M. Krygowski, and G. Merino, *Aromaticity and Antiaromaticity: Concepts and Applications* (New York: Wiley, 2022).

5. M. Solà, "Aromaticity rules," *Nature Chemistry* 14 (2022): 585–590.

6. E. Hückel, "Quantentheoretische Beiträge zum Benzolproblem," *Zeitschift für Physik* 70 (1931): 104–186.

7. a) R. Breslow, "Aromatic Character," *Chemical & Engineering News Archive* 43 (1965): 90–100. b) R. Breslow, "Antiaromaticity," *Accounts of Chemical Research* 6 (1973): 393–398.

8. N. C. Baird, "Quantum Organic Photochemistry. II. Resonance and Aromaticity in the Lowest $^3\pi\pi^*$ State of Cyclic Hydrocarbons," *Journal of the American Chemical Society* 94 (1972): 4941–4948.

9. a) H. Ottosson, "Exciting Excited-State Aromaticity," *Nature Chemistry* 4 (2012): 969–971. b) L. J. Karas and J. I. Wu, "Baird's Rules at the Tipping Point," *Nature Chemistry* 14 (2022): 723–725.

10. a) P. B. Karadakov, P. Hearnshaw, and K. E. Horner, "Magnetic Shielding, Aromaticity, Antiaromaticity, and Bonding in the Low-Lying Electronic States of Benzene and Cyclobutadiene," *Journal of Organic Chemistry* 81 (2016): 11346–11352. b) P. B. Karadakov and N. Preston, "Aromaticity Reversals and Their Effect on Bonding in the Low-Lying Electronic States of Cyclooctatetraene," *Physical Chemistry Chemical Physics* 23 (2021): 24750–24756.

11. T. Slanina, R. Ayub, J. Toldo, et al., "Impact of Excited-State Antiaromaticity Relief in a Fundamental Benzene Photoreaction Leading to Substituted Bicyclo[3.1.0]hexenes," *Journal of the American Chemical Society* 142 (2020): 10942–10954.

12. M. Ueda, K. Jorner, Y. M. Sung, et al., "Energetics of Baird Aromaticity Supported by Inversion of Photoexcited Chiral [4n]Annulene Derivatives," *Nature Communications* 8 (2017): 346.

13. G. Merino, M. Solà, I. Fernández, et al., "Aromaticity: Quo Vadis," *Chemical Science* 14 (2023): 5569–5576.

14. H. Ottosson, "A Focus on Aromaticity: Fuzzier Than Ever Before?," *Chemical Science* 14 (2023): 5542–5544.

15. J. Yan, T. Slanina, J. Bergman, and H. Ottosson, "Photochemistry Driven by Excited-State Aromaticity Gain or Antiaromaticity Relief," *Chemistry - A European Journal* 29 (2023): e202203748.

16. a) W. Zeng, O. El Bakouri, D. W. Szczepanik, H. Bronstein, and H. Ottosson, "Excited State Character of Cibalackrot-Type Compounds Interpreted in Terms of Hückel-Aromaticity: A Rationale for Singlet Fission Chromophore Design," *Chemical Science* 12 (2021): 6159–6171. b) W. Zeng, D. W. Szczepanik, and H. Bronstein, "Cibalackrot-Type Compounds: Stable Singlet Fission Materials With Aromatic Ground State and Excited State," *Journal of Physical Organic Chemistry* 36 (2023): e4441.

17. K. Jorner, F. Feixas, R. Ayub, R. Lindh, M. Solà, and H. Ottosson, "Analysis of a Compound Class With Triplet States Stabilized by Potentially Baird Aromatic [10]Annulenyl Dicationic Rings," *Chemistry - A European Journal* 22 (2016): 2793–2800.

18. S. Escayola, C. Tonellé, E. Matitio, et al., "Guidelines for Tuning the Excited State Hückel–Baird Hybrid Aromatic Character of Pro-Aromatic Quinoidal Compounds," *Angewandte Chemie, International Edition* 60 (2021): 10255–10265.

19. P. v. R. Schleyer, C. Maerker, A. Dransfeld, H. Jiao, and N. J. R. v. E. Hommes, "Nucleus-Independent Chemical Shifts: A Simple and Efficient Aromaticity Probe," *Journal of the American Chemical Society* 118 (1996): 6317–6318.

20. Z. Chen, C. S. Wannere, C. Corminboeuf, R. Puchta, and P. v. R. Schleyer, "Nucleus-Independent Chemical Shifts (NICS) as an Aromaticity Criterion," *Chemical Reviews* 105 (2005): 3842–3888.

21. L. M. Jackman, F. Sondheimer, Y. Amiel, et al., "The Nuclear Magnetic Resonance Spectroscopy of a Series of Annulenes and Dehydro-Annulenes," *Journal of the American Chemical Society* 84 (1962): 4307–4312.

22. S. Van Damme, G. Acke, R. W. A. Havenith, and P. Bultinck, "Can the Current Density Map Topology Be Extracted From the Nucleus Independent Chemical Shifts?," *Physical Chemistry Chemical Physics* 18 (2016): 11746–11755.

23. E. Paenurk and R. Gershoni-Poranne, "Simple and Efficient Visualization of Aromaticity: Bond Currents Calculated From NICS Values," *Physical Chemistry Chemical Physics* 24 (2022): 8631–8644.

24. P. Lazzaretti, "Assessment of Aromaticity Via Molecular Response Properties," *Physical Chemistry Chemical Physics* 6 (2004): 217–223.

25. P. Bultinck, S. Fias, and R. Ponec, "Local Aromaticity in Polycyclic Aromatic Hydrocarbons: Electron Delocalization Versus Magnetic Indices," *Chemistry - A European Journal* 12 (2006): 8813–8818.

26. A. Rehaman, A. Datta, S. S. Mallajosyula, and S. K. Pati, "Quantifying Aromaticity at the Molecular and Supramolecular Limits: Comparing Homonuclear, Heteronuclear, and H-Bonded Systems," *Journal of Chemical Theory and Computation* 2 (2006): 30–36.

27. Y.-C. Lin and D. Sundholm, "On the Aromaticity of the Planar Hydrogen-Bonded $(HF)_3$ Trimer," *Journal of Chemical Theory and Computation* 2 (2006): 761–764.

28. A. Banerjee, D. Halder, G. Ganguly, and A. Paul, "Deciphering the Cryptic Role of a Catalytic Electron in a Photochemical Bond Dissociation Using Excited State Aromaticity Markers," *Physical Chemistry Chemical Physics* 18 (2016): 25308–25314.

29. a) S. Fias, S. Van Damme, and P. Bultinck, "Multidimensionality of Delocalization Indices and Nucleus Independent Chemical Shifts in Polycyclic Aromatic Hydrocarbons," *Journal of Computational Chemistry* 29 (2008): 358–366. b) Z. Badri, S. Pathak, H. Fliegl, et al., "All-Metal Aromaticity: Revisiting the Ring Current Model Among Transition Metal Clusters," *Journal of Chemical Theory and Computation* 9 (2013): 4789–4796. c) A. Stanger, "The Seven-Membered Ring in Bis-Azuleno-Naphthalene Is Non-Aromatic," *European Journal of Organic Chemistry* 2019 (2019): 857–859.

30. D. Buzsáki, M. B. Kovács, E. Hümpfner, Z. Harcsa-Pintér, and Z. Kelemen, "Conjugation Between 3D and 2D Aromaticity: Does It Really Exist? The Case of Carborane-Fused Heterocycles," *Chemical Science* 13 (2022): 11388–11393.

31. T. Egawa, T. Fukuyama, S. Yamamoto, et al., "Molecular Structure and Puckering Potential Function of Cyclobutane Studied by Gas Electron Diffraction and Infrared Spectroscopy," *Journal of Chemical Physics* 86 (1987): 6018–6026.

32. E. M. Arpa and B. Durbeej, "HOMER: a Reparameterization of the Harmonic Oscillator Model of Aromaticity (HOMA) for Excited States," *Physical Chemistry Chemical Physics* 25 (2023): 16763–16771.

33. E. Steiner and P. W. Fowler, "Patterns of Ring Currents in Conjugated Molecules: A Few-Electron Model Based on Orbital Contributions," *Journal of Physical Chemistry. A* 105 (2001): 9553–9562.

34. M. J. Frisch, G. W. Trucks, H. B. Schlegel, et al., *Gaussian 16, Revision C.01* (Wallingford CT: Gaussian, Inc., 2016).

35. a) F. Neese, "Software Update: TheORCAprogram System—Version 5.0," *WIREs Computational Molecular Science* 12 (2022): e1606. b) F. Neese, A. Hansen, and D. G. Liakos, "Efficient and Accurate Approximations to the Local Coupled Cluster Singles Doubles Method Using a Truncated Pair Natural Orbital Basis," *Journal of Chemical Physics* 131 (2009): 064103. c) F. Neese, F. Wennmohs, and A. Hansen, "Efficient and Accurate Local Approximations to Coupled-Electron Pair Approaches: An Attempt to Revive the Pair Natural Orbital Method," *Journal of Chemical Physics* 130 (2009): 114108. d) C. Riplinger and F. Neese, "An Efficient and Near Linear Scaling Pair Natural Orbital Based Local Coupled Cluster Method," *Journal of Chemical Physics* 138 (2013): 034106. e) C. Riplinger, B. Sandhoefer, A. Hansen, and F. Neese, "Natural Triple Excitations in Local Coupled Cluster Calculations With Pair Natural Orbitals," *Journal of Chemical Physics* 139 (2013): 134101. f) C. Riplinger, P. Pinski, U. Becker, E. F. Valeev, and F. Neese, "Sparse Maps—A Systematic Infrastructure for Reduced-Scaling Electronic Structure Methods. II. Linear Scaling Domain Based Pair Natural Orbital Coupled Cluster Theory," *Journal of Chemical Physics* 144 (2016): 024109. g) G. Bistoni, C. Riplinger, Y. Minenkov, L. Cavallo, A. A. Auer, and F. Neese, "Treating Subvalence Correlation Effects in Domain Based Pair Natural Orbital Coupled Cluster Calculations: An Out-of-the-Box Approach," *Journal of Theoretical and Computational Chemistry* 13 (2017): 3220–3227. h) F. Neese, "The SHARK integral generation and digestion system," *Journal of Computational Chemistry* 44 (2023): 381–396.

36. a) P. J. Stephens, F. J. Devlin, C. F. Chabalowski, and M. J. Frisch, "Ab Initio Calculation of Vibrational Absorption and Circular Dichroism Spectra Using Density Functional Force Fields," *Journal of Physical Chemistry* 98 (1994): 11623–11627. b) R. Krishnan, K. S. Binkley, R. Seeger, and J. A. Pople, "Self-Consistent Molecular Orbital Methods. XX. A Basis Set for Correlated Wave Functions," *Journal of Chemical Physics* 72 (1980): 650–654.

37. A. Stanger, "Obtaining Relative Induced Ring Currents Quantitatively From NICS," *Journal of Organic Chemistry* 75 (2010): 2281–2288.

38. R. Gershoni-Poranne and A. Stanger, "The NICS-XY-Scan: Identification of Local and Global Ring Currents in Multi-Ring Systems," *Chemistry - A European Journal* 20 (2014): 5673–5688.

39. R. Gershoni-Poranne and A. Stanger, *Aromaticity: Modern Computational Methods and Applications*, ed. I. Fernández (Amsterdam: Elsevier, 2021) Ch.4.

40. D. Geuenich, K. Hess, F. Köhler, and R. Herges, "Anisotropy of the Induced Current Density (ACID), a General Method to Quantify and Visualize Electronic Delocalization," *Chemical Reviews* 105 (2005): 3758–3772.

41. G. Monaco, F. F. Summa, and R. Zanasi, "Program Package for the Calculation of Origin-Independent Electron Current Density and Derived Magnetic Properties in Molecular Systems," *Journal of Chemical Information and Modeling* 61 (2021): 270–283.

42. E. Matito, M. Duran, and M. Solà, "The Aromatic Fluctuation Index (FLU): A New Aromaticity Index Based on Electron Delocalization," *Journal of Chemical Physics* 122 (2005): 014109.

43. P. Bultinck, R. Ponec, and S. Van Damme, "Multicenter Bond Indices as a New Measure of Aromaticity in Polycyclic Aromatic Hydrocarbons," *Journal of Physical Organic Chemistry* 18 (2005): 706–718.

44. a) J. Kruszewski and T. M. Krygowski, "Definition of Aromaticity Basing on the Harmonic Oscillator Model," *Tetrahedron Letters* 13 (1972): 3839–3842. b) T. M. Krygowski, H. Szatylowicz, O. A. Stasyuk, J. Dominikowska, and M. Palusiak, "Aromaticity From the Viewpoint of Molecular Geometry: Application to Planar Systems," *Chemical Reviews* 114 (2014): 6383–6422.

45. a) K. Aidas, C. Angeli, K. L. Bak, et al., "The Dalton Quantum Chemistry Program System," *WIREs Computational Molecular Science* 4 (2014): 269–284. b) *Dalton, a Molecular Electronic Structure Program, Release v2016.2* (2017), see http://daltonprogram.org.

46. A. Stanger, "NICS – Past and Present," *European Journal of Organic Chemistry* 2020 (2020): 3120–3127.

47. A. Stanger, "Nucleus Independent Chemical Shift (NICS) at Small Distances From the Molecular Plane: The Effect of Electron Density," *ChemPhysChem* 24 (2023): e202300080.

48. a) L. Nyulászi and P. v. R. Schleyer, "Hyperconjugative π-Aromaticity: How to Make Cyclopentadiene Aromatic," *Journal of the American Chemical Society* 121 (1999): 6872–6875. b) A. Stanger, "Can Substituted Cyclopentadiene Become Aromatic or Antiaromatic?," *Chemistry - A European Journal* 12 (2006): 2745–2751. c) K. Jorner, R. Emanuelsson, C. Dahlstrand, H. Tong, A. V. Denisova, and H. Ottosson, "Analysis of a Compound Class With Triplet States Stabilized by Potentially Baird Aromatic [10]Annulenyl Dicationic Rings," *Chemistry - A European Journal* 20 (2014): 9295–9303.

49. J. Trotter, "The Crystal and Molecular Structure of Biphenyl," *Acta Cryst* 14 (1961): 1135–1140.

50. M. Rubio, M. Merchán, E. Ortí, and B. O. Roos, "A Theoretical Study of the Electronic Spectrum of Biphenyl," *Chemical Physics Letters* 234 (1995): 373–381.

51. R. Fukuda and M. Ehara, "Electronic Excited States and Electronic Spectra of Biphenyl: A Study Using Many-Body Wavefunction Methods and Density Functional Theories," *Physical Chemistry Chemical Physics* 15 (2013): 17426–17434.

52. a) Y. Carissan, D. Hagebaum-Reignier, N. Goudard, and S. Humbel, "Hückel-Lewis Projection Method: A 'Weights Watcher' for Mesomeric Structures," *Journal of Physical Chemistry. A* 112 (2008): 13256–13262. b) Y. Carissan, D. Hagebaum-Reignier, N. Goudard, S. Humbel, *HuLiS Program: Lewis Embedded in Hückel Theory* (2008), http://www.hulis.free.fr; c) Y. Carissan, D. Hagebaum-Reignier, N. Goudard, and S. Humbel, "Weight Watchers électronique : calculez votre poids de formes résonantes," *L'Actualité Chimique* 406 (2016): 36–40.

53. R. Ayub, O. El Bakouri, K. Jorner, M. Solà, and H. Ottosson, "Can Baird's and Clar's Rules Combined Explain Triplet State Energies of Polycyclic Conjugated Hydrocarbons With Fused 4nπ- and (4n+2)π-Rings?," *Journal of Organic Chemistry* 82 (2017): 6327–6340.

54. M. Rosenberg, C. Dahlstrand, K. Kilså, and H. Ottosson, "Excited State Aromaticity and Antiaromaticity: Opportunities for Photophysical and Photochemical Rationalizations," *Chemical Reviews* 114 (2014): 5379–5425.

55. N. S. Mills and K. B. Llagostera, "Summation of Nucleus Independent Chemical Shifts as a Measure of Aromaticity," *Journal of Organic Chemistry* 72 (2007): 9163–9169.

56. B. O. Roos, P. R. Taylor, and P. E. M. Siegbahn, "A Complete Active Space SCF Method (CASSCF) Using a Density Matrix Formulated Super-CI Approach," *Chemical Physics* 48 (1980): 157–173.

57. a) W. J. Buma, J. H. van der Waals, and M. C. van Hemert, "Conformational Instability of the Lowest Triplet State of the Benzene Nucleus. I. The Unsubstituted Molecule," *Journal of Chemical Physics* 93 (1990): 3733–3745. b) N. Zamstein, S. Kallush, and B. J. Segev, "A Phase-Space Approach to the T1⇝S Radiationless Decay in Benzene: The Effect of Deuteration," *Chemical Physics* 123 (2005): 074304.

Supporting Information

Additional supporting information can be found online in the Supporting Information section.